Spectral broadening effects of spontaneous emission and density of state on plasmonic enhancement in cermet waveguides

Keyong Chen, Xue Feng,* Chao Zhang, Kaiyu Cui, and Yidong Huang

Department of Electronic Engineering, State Key Laboratory of Integrated Optoelectronics, Tsinghua University, Beijing 100084, China
**x-feng@tsinghua.edu.cn*

Abstract: Based on the full integration formula of Purcell factor (PF) deduced from Fermi's Golden Rule, the plasmonic enhancement in Au(1-α)Si_3N_4(α) cermet waveguides is evaluated with the joint impact of finite emission linewidth and the broadening of PF spectrum. The calculation results indicate that the PF would be significantly degraded by the two broadening effects though the SPP resonance frequency can be tuned with different volume fractions (α) of Si_3N_4. It is also found that the critical emission linewidth is approximately linear to the PF spectrum linewidth. Thus in order to achieve strong plasmonic enhancement, both the emission and PF spectrum linewidths should be dramatically reduced.

OCIS codes: (240.6680) Surface plasmons; (130.2790) Guided waves; (310.3915) Metallic, opaque, and absorbing coatings.

References and links

1. A. V. Zayats, I. I. Smolyaninov, and A. A. Maradudin, "Nano-optics of surface plasmon polaritons," Phys. Rep. **408**(3-4), 131–314 (2005).
2. M. Gontijo, M. Boroditsky, E. Yablonovitch, S. Keller, U. Mishra, and S. DenBaars, "Coupling of InGaN quantum-well photoluminescence to silver surface plasmons," Phys. Rev. B **60**(16), 11564–11567 (1999).
3. K. Okamoto, I. Niki, A. Shvartser, Y. Narukawa, T. Mukai, and A. Scherer, "Surface-plasmon-enhanced light emitters based on InGaN quantum wells," Nat. Mater. **3**(9), 601–605 (2004).
4. C. W. Lai, J. An, and H. C. Ong, "Surface-plasmon-mediated emission from metal-capped ZnO thin films," Appl. Phys. Lett. **86**(25), 251105 (2005).
5. J. S. Biteen, D. Pacifici, N. S. Lewis, and H. A. Atwater, "Enhanced radiative emission rate and quantum efficiency in coupled silicon nanocrystal-nanostructured gold emitters," Nano Lett. **5**(9), 1768–1773 (2005).
6. Y. Y. Gong, J. Lu, S. L. Cheng, Y. Nishi, and J. Vučković, "Plasmonic enhancement of emission from Si-nanocrystals," Appl. Phys. Lett. **94**(1), 013106 (2009).
7. K. Okamoto, A. Scherer, and Y. Kawakami, "Surface plasmon enhanced light emission from semiconductor materials," Phys. Status Solidi C **5**(9), 2822–2824 (2008).
8. F. Hatami, V. Lordi, J. S. Harris, H. Kostial, and W. T. Masselink, "Red light-emitting diodes based on InP/GaP quantum dots," J. Appl. Phys. **97**(9), 096106 (2005).
9. H. Yokoyama and K. Ujihara, eds., *Spontaneous Emission and Laser Oscillation in Microcavities* (CRC, 1995), Chap. 8.
10. E. M. Purcell, H. C. Torrey, and R. V. Pound, "Resonance absorption by nuclear magnetic moments in a solid," Phys. Rev. **69**(1-2), 37–38 (1946).
11. X. Hu, Y. Huang, W. Zhang, and J. Peng, "Dominating radiative recombination in a nanoporous silicon layer with a metal-rich Au(1-α)SiO_2(α) cermet waveguide," Appl. Phys. Lett. **89**(8), 081112 (2006).
12. X. Tang, Y. Wang, W. Ke, X. Feng, Y. Huang, and J. Peng, "Internal quantum efficiency enhancement of silicon nanocrystals using double layer Au-rich cermet films," Opt. Commun. **283**(13), 2754–2757 (2010).
13. D. Lu, J. Kan, E. E. Fullerton, and Z. Liu, "Tunable surface plasmon polaritons in Ag composite films by adding dielectrics or semiconductors," Appl. Phys. Lett. **98**(24), 243114 (2011).
14. X. Feng, F. Liu, and Y. D. Huang, "Calculated plasmonic enhancement of spontaneous emission from silicon nanocrystals with metallic gratings," Opt. Commun. **283**(13), 2758–2761 (2010).
15. X. Feng, F. Liu, and Y. D. Huang, "Spontaneous emission rate enhancement of silicon nanocrystals by plasmonic bandgap on copper grating," J. Lightwave Technol. **28**(9), 1420–1430 (2010).
16. G. Sun, J. B. Khurgin, and R. A. Soref, "Practicable enhancement of spontaneous emission using surface plasmons," Appl. Phys. Lett. **90**(11), 111107 (2007).
17. J. T. Robinson, C. Manolatou, L. Chen, and M. Lipson, "Ultrasmall mode volumes in dielectric optical microcavities," Phys. Rev. Lett. **95**(14), 143901 (2005).

#176746 - $15.00 USD Received 24 Sep 2012; revised 14 Nov 2012; accepted 9 Dec 2012; published 4 Jan 2013

18. P. Cheng, D. Li, Z. Yuan, P. Chen, and D. Yang, "Enhancement of ZnO light emission via coupling with localized surface plasmon of Ag island film," Appl. Phys. Lett. **92**(4), 041119 (2008).
19. C. Hong, H. Kim, S. Park, and C. Lee, "Optical properties of porous silicon coated with ultrathin gold film by RF-magnetron sputtering," J. Eur. Ceram. Soc. **30**(2), 459–463 (2010).
20. M. van Exter, G. Nienhuis, and J. Woerdman, "Two simple expressions for the spontaneous emission factor β," Phys. Rev. A **54**(4), 3553–3558 (1996).
21. T. Baba and D. Sano, "Low-threshold lasing and Purcell effect in microdisk lasers at room temperature," IEEE J. Sel. Top. Quantum Electron. **9**(5), 1340–1346 (2003).
22. H. Iwase, D. Englund, and J. Vučković, "Analysis of the Purcell effect in photonic and plasmonic crystals with losses," Opt. Express **18**(16), 16546–16560 (2010).
23. X. Feng, K. Cui, F. Liu, and Y. Huang, "Impact of spectral broadening on plasmonic enhancement with metallic gratings," Appl. Phys. Lett. **101**(12), 121102 (2012).
24. Y. Gong and J. Vučković, "Design of plasmon cavities for solid-state cavity quantum electrodynamics applications," Appl. Phys. Lett. **90**(3), 033113 (2007).
25. P. Milonni, *The Quantum Vacuum: An Introduction to Quantum Electrodynamics* (Academic, 1994).
26. P. Sheng, "Theory for the dielectric function of granular composite media," Phys. Rev. Lett. **45**(1), 60–63 (1980).
27. U. J. Gibson and R. A. Buhrman, "Optical response of cermet composite films in the microstructural transition region," Phys. Rev. B **27**(8), 5046–5051 (1983).
28. T. Bååk, "Silicon oxynitride; a material for GRIN optics," Appl. Opt. **21**(6), 1069–1072 (1982).
29. W. Chen, M. D. Thoreson, A. V. Kildishev, and V. M. Shalaev, "Fabrication and optical characterizations of smooth silver-silica nanocomposite films," Laser Phys. Lett. **7**(9), 677–684 (2010).
30. N. C. Miller, B. Hardiman, and G. A. Shirn, "Transport properties, microstructure, and conduction model of cosputtered Au-SiO_2 cermet films," J. Appl. Phys. **41**(4), 1850–1856 (1970).
31. J. J. Burke, G. I. Stegeman, and T. Tamir, "Surface-polariton-like waves guided by thin, lossy metal films," Phys. Rev. B Condens. Matter **33**(8), 5186–5201 (1986).
32. R. R. Chance, A. Prock, and R. Silbey, "Molecular fluorescence and energy transfer near interfaces," Adv. Chem. Phys. **37**, 1–65 (1978).
33. G. W. Ford and W. H. Weber, "Electromagnetic interactions of molecules with metal surfaces," Phys. Rep. **113**(4), 195–287 (1984).
34. W. L. Barnes, "Electromagnetic crystals for surface plasmon polaritons and the extraction of light from emissive devices," J. Lightwave Technol. **17**(11), 2170–2182 (1999).

1. Introduction

Surface plasmon polariton (SPP) is a transverse-magnetic (TM) surface electromagnetic excitation propagating along the metal-dielectric interface [1] and has attracted much attention to enhance the spontaneous emission (fluorescence) efficiencies of light emitters with various active materials from wide-band-gap semiconductors, such as InGaN/GaN [2,3] and ZnO [4], to narrow-band-gap semiconductors such as InP or Si quantum dots (QDs) [5–8]. According to Fermi's Golden Rule [9], the large density of state (DOS) for SPP mode near the resonance frequency could dramatically enhance the recombination rate of spontaneous emission (SE) coupled into SPP mode, which is well known as the Purcell effect that modifies the SE by engineering the dispersion [10]. Up to now, there has been much progress in effectively utilizing SPP waveguides to enhance the SE rate. The effects of different metal films including Au, Ag and Al were experimentally demonstrated and compared on the light emission of InGaN quantum wells by Koichi Okamoto et al. [3]. Cermet waveguides doped with dielectric were introduced to tune the SPP resonance to lower frequencies for the narrow-gap semiconductors in our previous work [11,12] and by Dylan Lu et al. [13]. Furthermore, we have proposed metallic gratings of Au, Ag and Al, and even Cu which is the mainstay metallic material in microelectronic chips, to enhance the SE rate of Si-nanocrystals whose emission frequency range is as low as 1.6~1.9eV [14,15]. In these researches, Purcell factor (PF) is the most popular figure of merit to evaluate the plasmonic enhancement and in general, it is derived from the reduced form of Fermi's Golden Rule, where yet only the DOS and the mode volume (namely the effect of cavity or SPP waveguide) are involved [2,6,11,12,14–16]. However, such a treatment is based on the assumption that the emission linewidth of emitter is sufficiently narrow [9,17], which actually disregards the influence of SE spectrum. For practical emitters, the typical emission linewidth range may be as broad as 0.1~1.0 eV according to previous experimental reports [2,3,5–7,18,19]. Thus, the impact of emission linewidth should be considered in the evaluation of plasmonic enhancement or otherwise the PF and the SE rate into SPP mode would be remarkably overestimated [20,21]. On the other hand, the waveguide absorption loss could give rise to the broadening and

#176746 - $15.00 USD Received 24 Sep 2012; revised 14 Nov 2012; accepted 9 Dec 2012; published 4 Jan 2013

degradation of DOS spectrum and consequently PF spectrum [22]. Because of this concurrent effect, the joint impact of finite SE and PF spectrum linewidths on plasmonic enhancement becomes more interesting. In our previous work, the interaction between such two linewidths was clarified based on metallic gratings [23] and now, we would like to extend our discussion into cermet waveguides with uniform interfaces.

In this paper, a full integration formula of PF for smooth SPP waveguides is firstly deduced from Fermi's Golden Rule while the SE and DOS spectra are involved. By taking Au(1-α)Si_3N_4(α) cermet waveguide for example, the cermet permittivity, dispersion curves and electric field distributions are calculated under the air/waveguide/emitter structure to obtain the corresponding PF. The capability of tuning the SPP resonance frequency (ω_{sp}) is then demonstrated for the cermet with different volume fraction (α) of Si_3N_4. The tuning range is $\hbar\omega_{sp}$ = 2.48~1.765 eV with α = 0~0.3, where α = 0 denotes pure Au without any doping. Afterwards, the PF spectra based on the reduced formula are numerically calculated at different vertical locations in the emitter before the impact of emission linewidth is introduced. It is found that the PF spectrum is degraded and broadened with increasing distance from the cermet-emitter interface and its central frequency is also decreased, as in Ref [22]. After taking into account the SE spectrum of emitter, the PFs in the full integral form at different locations are calculated and averaged over the active layer to evaluate the overall plasmonic enhancement with varied emission linewidths (10^{-3}~10^6 meV). It is found that the enhancement decreases significantly when the emission linewidth exceeds ~0.1 eV which, however, is commonly adopted in the previous experiments [2,3,5–7,18,19]. Furthermore, to illustrate when the emission linewidth is "sufficiently narrow" for achieving strong plasmonic enhancement, we define the critical emission linewidth ($\Delta\omega$*) as the one where the average PF (PF_{ave}) drops to half of its maximum. It is found that $\Delta\omega$* has an approximately linear relation with the linewidth of PF spectrum at the surface of the emitter ($\Delta\omega_{PF}$). Based on this relation, $\Delta\omega$* can be readily estimated and the emission linewidth is supposed to be sufficiently narrow when it is less than $\Delta\omega$*. However, in order to obtain ultrahigh enhancement (PF_{ave}>100), the PF spectrum linewidth still needs to be reduced by decreasing the propagation loss of SPP mode.

2. Full integration formula of Purcell factor

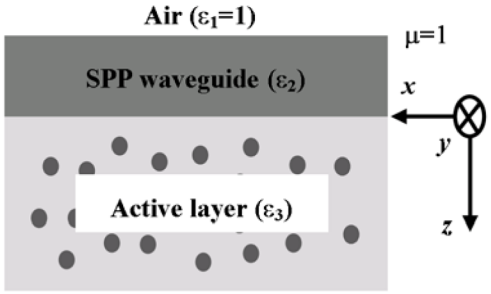

Fig. 1. Schematic diagram of a SPP waveguide on the uniformly distributed QDs active layer in an air/waveguide/emitter structure, and reference coordinate system.

Figure 1 is the schematic setup of the SPP waveguide on top of the active layer, in which mass QDs serve as the light emitter. ε_1, ε_2 and ε_3 are the permittivities of the air (ε_1 = 1), the SPP waveguide and the active layer, respectively. The permeabilities of all media are set μ = 1. According to Fermi's Golden Rule, the SE rate Γ_{sp} is [9]:

$$\Gamma_{sp} = \frac{2\pi}{\hbar}\int_0^\infty \left|\langle f|\boldsymbol{d}\cdot\boldsymbol{E}(\boldsymbol{r})|i\rangle\right|^2 \cdot \rho(\omega)\cdot\ell(\omega)d\omega, \quad (1)$$

#176746 - $15.00 USD Received 24 Sep 2012; revised 14 Nov 2012; accepted 9 Dec 2012; published 4 Jan 2013

where $\langle f|\boldsymbol{d}\cdot\boldsymbol{E}(\boldsymbol{r})|i\rangle$ is the dipole emission matrix element, $\boldsymbol{d}$ is the electro-hole pair dipole moment, $\boldsymbol{E}(\boldsymbol{r})$ is the electric field distribution, ω is the angular frequency and $\hbar$ is the reduced Planck constant. $\rho(\omega)$ is the DOS for SPP mode and $\ell(\omega)$ is the mode density of dipole transition or SE spectrum with the normalization condition $\int_0^\infty \ell(\omega)d\omega = 1$. Usually, the ensemble emission linewidth of mass QDs is wider than that of single QD due to the size non-uniformity. In principle, the size distribution of QDs could be reduced by optimized fabrication process, so we assume that the sizes of all QDs are the same and thus only the linewidth of SE from single QD is considered. Suppose that the homogeneous broadening is dominant, the SE spectrum for single QD could be expressed as Lorentzian function [9]:

$$\ell(\omega-\omega_0) = \frac{\Delta\omega/2\pi}{(\omega-\omega_0)^2+(\Delta\omega/2)^2}, \tag{2}$$

where ω_0 is the central emission frequency and $\Delta\omega$ is the emission linewidth. If $\Delta\omega$ is much narrower than that of $\rho(\omega)$, Eq. (1) could be reduced to:

$$\Gamma_{sp}(\omega_0) = \frac{2\pi}{\hbar}\left|\langle f|\boldsymbol{d}\cdot\boldsymbol{E}(\boldsymbol{r})|i\rangle\right|^2\cdot\rho(\omega_0). \tag{3}$$

Equation (3) is commonly used to evaluate the plasmonic enhancement [2,6,11,12,14–16,22,24]. However, for a practical emitter with finite emission linewidth, Eq. (1) should be employed. In addition, it has been found that the DOS spectrum of SPP mode would also be broadened due to the waveguide absorption loss and could also be expressed as Lorentzian function [22,24]:

$$\rho(\omega-\omega_k) = \frac{\omega_k/2\pi Q_k}{(\omega-\omega_k)^2+(\omega_k/2Q_k)^2}, \tag{4}$$

where ω_k and Q_k are the frequency and the quality factor for state k, respectively. Thus the SE rate should be the sum of the rates for all k states under specific ω_0:

$$\Gamma_{sp}(\omega_0) = \int_0^\infty \sum_k \frac{2\pi}{\hbar^2}\left|\langle f|\boldsymbol{d}\cdot\boldsymbol{E}_k(\boldsymbol{r})|i\rangle\right|^2\cdot\rho(\omega-\omega_k)\cdot\ell(\omega-\omega_0)d\omega. \tag{5}$$

For simplicity, we start from the reduced form of Γ_{sp} to deduce the PF. Firstly, $\left|\langle f|\boldsymbol{d}\cdot\boldsymbol{E}_k|i\rangle\right|^2$ is rewritten as $1/3(d^2|E_k|^2)$ with an averaging factor of 1/3 for the random polarization direction of $\boldsymbol{d}$ to $\boldsymbol{E}_k$, as in Ref [2]. $\boldsymbol{E}_k$ is normalized to a half quantum for zero-point fluctuations within a prepared space of $V = L_xL_yL_z$:

$$|E_k|^2 = \frac{\hbar\omega/2\cdot|E_0^k(r)|^2}{1/8\pi\int^{L_x}\int^{L_y}\int^{L_z}[\partial(\varepsilon\omega_k)/\partial\omega_k]\cdot|E_0^k(x,y,z)|^2dxdydz}, \tag{6}$$

where E_0^k is the original electric field for state k, and ε is the frequency-dependent permittivity that also varies with different locations in the air/waveguide/emitter structure. What's more, the integration along z direction is $L_z\to\pm\infty$ and in x and y directions, $\boldsymbol{E}_k$ is homogeneous so the denominator or stored energy is rewritten as $L_xL_y/(8\pi)\cdot\int_{-\infty}^{+\infty}[\partial(\varepsilon\omega_k)/\partial\omega_k]|E_0^k(z)|^2dz$. In the reciprocal space, the mode area of one SPP mode could be expressed as $\Delta k_x\Delta k_y = (2\pi)^2/L_xL_y$. Then the SE rate for state k based on Eqs. (3)–(6) is obtained:

#176746 - $15.00 USD Received 24 Sep 2012; revised 14 Nov 2012; accepted 9 Dec 2012; published 4 Jan 2013

$$\Gamma_{sp}^{k}(\omega_0)=\frac{2d^2\omega_0}{3\hbar}\cdot\frac{\left|E_0^k(z)\right|^2}{\int_{-\infty}^{+\infty}\left[\partial(\varepsilon\omega_k)/\partial\omega_k\right]\left|E_0^k(z)\right|^2dz}\cdot\rho(\omega_0-\omega_k)\Delta k_x\Delta k_y. \tag{7}$$

This recombination rate should be compared to the SE rate $\Gamma_0(\omega_0)$ in bulk semiconductors, which is calculated by the classical equation [25]:

$$\Gamma_0(\omega)=\frac{4nd^2\omega^3}{3\hbar c^3}, \tag{8}$$

where c is the vacuum speed of light and n is the refractive index of active layer. With Eqs. (7) and (8), the reduced formula of PF is deduced as [2]:

$$PF(z\,|\,\omega_0)=1+\sum_k\frac{\Gamma_{sp}^k(\omega_0)}{\Gamma_0(\omega_0)}=1+\frac{c^3}{2n\omega_0^2}\sum_k\frac{\left|E_0^k(z)\right|^2}{\int_{-\infty}^{+\infty}\left[\partial(\varepsilon\omega_k)/\partial\omega_k\right]\left|E_0^k(z)\right|^2dz}\cdot\rho(\omega_0-\omega_k)\Delta k_x\Delta k_y. \tag{9}$$

If the real space is large enough, k_x and k_y could be treated as continuous variables and $\sum_k\Delta k_x\Delta k_y$ approximates $\int_{-\infty}^{+\infty}\int_{-\infty}^{+\infty}dk_xdk_y$. Then by integrating $PF(z\,|\,\omega_0)$ in polar coordinates $\boldsymbol{k}=(k\cos\phi,k\sin\phi,0)$, $\int_{-\infty}^{+\infty}\int_{-\infty}^{+\infty}dk_xdk_y$ is rewritten as $\int_0^{2\pi}\int_0^{\infty}kdkd\phi$ where k is the propagation constant, independent of ϕ. So taking the SE spectrum into account, we obtain the PF in the full integral form:

$$PF(z\,|\,\omega_0)=1+\frac{\pi c^3}{n\omega_0^2}\int_0^{\infty}\int_0^{\infty}H(\omega_k)\cdot\rho(\omega-\omega_k)\cdot\ell(\omega-\omega_0)\frac{kdk}{d\omega_k}d\omega_kd\omega, \tag{10}$$

where $H(\omega_k)=\left|E_0^k(z)\right|^2\Big/\int_{-\infty}^{+\infty}\left[\partial(\varepsilon\omega_k)/\partial\omega_k\right]\left|E_0^k(z)\right|^2dz$. It should be noted that $d\omega_k$ replaces dk as the integration variable by multiplying $dk/d\omega_k$ for convenient calculation of PF because both $\rho(\omega)$ and l(ω) are explicit functions of ω.

Till now, the full integration formula of PF has been obtained. To verify this formula, we consider two special cases. First, if the emission linewidth ($\Delta\omega$) is sufficiently narrow, l(ω–ω_0) would be Dirac's function $\delta(\omega-\omega_0)$. Thus Eq. (10) is reduced to:

$$PF(\omega_0,z)=1+\frac{\pi c^3}{n\omega_0^2}\int_0^{\infty}H(\omega_k)\cdot\rho(\omega_0-\omega_k)\frac{kdk}{d\omega_k}d\omega_k \tag{11}$$

which is the PF spectrum, consistent with the formula in Ref [22]. Second, if absorption loss of the SPP waveguide is neglected, $\rho(\omega_0-\omega_k)$ would also be Dirac's function $\delta(\omega_0-\omega_k)$ so that Eq. (11) could be further simplified to $PF(\omega_0,z)=1+\frac{\pi c^3}{n\omega_0^2}\cdot H(\omega_0)\cdot\frac{kdk}{d\omega_0}$, which is the commonly used formula to evaluate the plasmonic enhancement [2,6,11,12,14–16].

3. Permittivity of cermet waveguides

To analyze the plasmonic enhancement quantitatively, we consider a representative SPP waveguide based on cermet of Au(1-α)Si_3N_4(α), where α is the volume fraction of Si_3N_4 and α = 0 denotes pure Au. The cermet permittivity (ε_2) is derived from the probabilistic growth model introduced by Sheng [26,27]:

#176746 - $15.00 USD Received 24 Sep 2012; revised 14 Nov 2012; accepted 9 Dec 2012; published 4 Jan 2013

$$p\frac{\varepsilon_{MetalCoat}-\varepsilon_2}{\varepsilon_{MetalCoat}+2\varepsilon_2}+(1-p)\frac{\varepsilon_{DielectricCoat}-\varepsilon_2}{\varepsilon_{DielectricCoat}+2\varepsilon_2}=0, \tag{12}$$

where the cermet material is modeled as a mixture of two types of coated spheres (i.e., metal-coated dielectric sphere and dielectric-coated metal sphere) with respective dielectric functions:

$$\varepsilon_{MetalCoat}=\frac{\varepsilon_M(2\alpha(\varepsilon_D-\varepsilon_M)+(\varepsilon_D+2\varepsilon_M))}{(\varepsilon_D+2\varepsilon_M)-\alpha(\varepsilon_D-\varepsilon_M)}, \tag{13}$$

$$\varepsilon_{DielectricCoat}=\frac{\varepsilon_D(2(1-\alpha)(\varepsilon_M-\varepsilon_D)+(\varepsilon_M+2\varepsilon_D))}{(\varepsilon_M+2\varepsilon_D)-(1-\alpha)(\varepsilon_M-\varepsilon_D)}, \tag{14}$$

and the probability of forming a metal-coated dielectric sphere is:

$$p=\frac{(1-\alpha^{1/3})^3}{(1-\alpha^{1/3})^3+(1-(1-\alpha)^{1/3})^3}. \tag{15}$$

ε_M and ε_D are the permittivities of Au metal and Si_3N_4 dielectric, respectively.

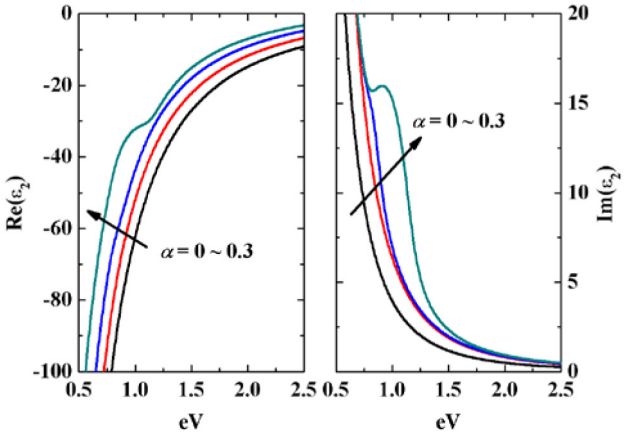

Fig. 2. Calculated permittivity of different Au(1-α)Si_3N_4(α) cermet with α = 0, 0.1, 0.2 and 0.3, respectively.

Compared with SiO_2 adopted in our previous work [11], the refractive index of Si_3N_4 is higher so that the SPP resonance could be tuned in a wider frequency range. The frequency-dependent permittivity of Si_3N_4 is taken from Ref [28]. The permittivity of Au is given by $\varepsilon_M=1-\omega_M^2/(\omega^2+i\omega/\tau_M)$ with the plasma frequency $\omega_M = 1.21 \times 10^{16}$ sec^{-1} and the plasma life-time $\tau_M = 1.05 \times 10^{-14}$ sec [22]. Because the grain size effect of Au nanoclusters (Au-NCs) should also be considered for the cermet, the plasma life-time should be modified by introducing a correction term as: $1/\tau_{M*} = 1/\tau_M + A \times v_F/R$, where v_F is the Fermi velocity equal to 1.39×10^6 m/s, R is the average Au-NC radius, and A is the parameter related to the scattering processes and the type of dielectric surrounding the Au-NC, with a value of around one [29]. Accordingly, we assume A = 1 and estimate R to be 16.3 nm (α = 0.1), 11.2 nm (α = 0.2) and 7.9 nm (α = 0.3), based on the power function $R = 24.53 \times (1+\alpha)^{-4.32}$ which is obtained by fitting the experimental data from Ref [30]. Figure 2 shows the calculated permittivity of Au(1-α)Si_3N_4(α) cermet with α = 0~0.3. The real part of the cermet permittivity (Re(ε_2)) remains negative, so the cermet is also regarded as metallic material and can sustain the propagating SPP mode.

#176746 - $15.00 USD Received 24 Sep 2012; revised 14 Nov 2012; accepted 9 Dec 2012; published 4 Jan 2013

4. Spectral broadening effects of SE and DOS on plasmonic enhancement

Before calculating the PF, it is necessary to acquire the dispersion curves and the electric field distributions of SPP mode propagating on the Au(1-α)Si_3N_4(α) cermet waveguide in order to calculate the DOS and the normalized electric field. Firstly, we assume that the active material is InP QDs embedded in GaP [8] with refractive index of n = 3. The thickness of the cermet layer is set 10 nm. Then the complex propagation constant (k_{sp} = k-ik'') of SPP mode can be calculated by the following dispersion relation of TM mode [31]:

$$\tan h(\gamma_2 h)(\varepsilon_1\varepsilon_3\gamma_2^2+\varepsilon_2^2\gamma_1\gamma_3)+[\gamma_2(\varepsilon_1\gamma_3+\varepsilon_3\gamma_1)\varepsilon_2]=0, \qquad (16)$$

where $\gamma_j^2 = k_{sp}^2 - \varepsilon_j k_0^2$, j = 1, 2, 3, respectively. k_0 is the wave vector in vacuum and h is the thickness of the cermet layer.

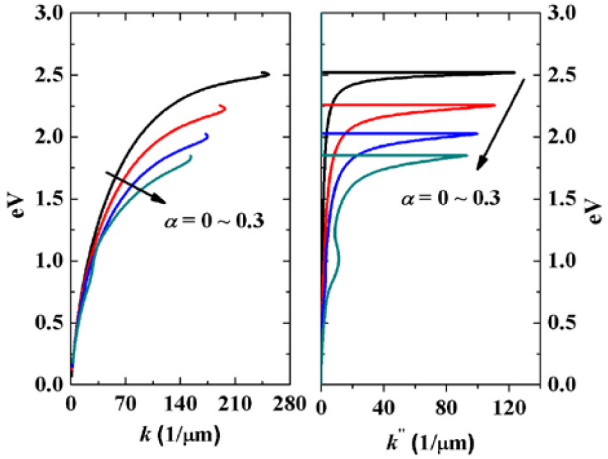

Fig. 3. Dispersion curves of SPP mode on different Au(1-α)Si_3N_4(α) cermet waveguides with α = 0~0.3.

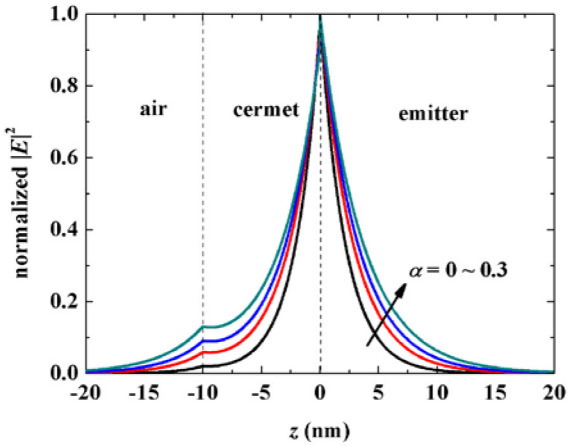

Fig. 4. Normalized distributions of electric field along z at SPP resonance frequencies for α = 0~0.3.

Figure 3 shows the calculated dispersion cures with α = 0~0.3. It should be noted that for each α, there are two branches of SPP mode (i.e., anti-symmetric and symmetric branches), but only anti-symmetric SPP mode is considered here because the symmetric one is a leaky

#176746 - $15.00 USD Received 24 Sep 2012; revised 14 Nov 2012; accepted 9 Dec 2012; published 4 Jan 2013

mode at low frequencies and therefore cannot be exploited [11]. With increasing α, SPP resonance is tuned to lower frequency (the corresponding resonance energies are 2.48 eV, 2.18 eV, 1.945 eV and 1.765 eV, respectively). On the other hand, the electric field distribution can be calculated from Maxwell's equations and boundary conditions of continuity [29]. Figure 4 shows the normalized distributions of electric field along z ($\left|E_0^k(z)\right|^2 \Big/ \max\left(\left|E_0^k(z)\right|^2\right)$) at the resonance energies for different α. The field intensities in the emitter decay exponentially away from the waveguide. They are primarily localized at the cermet-emitter interface contributing to greater plasmonic enhancement at the SPP resonance frequencies. With increasing α the field distribution expands along z. After the dispersion curves are obtained, the DOS can be calculated with Eq. (4) where Q_k equals $\omega_k/(2k'' \times \mathrm{d}\omega_k/\mathrm{d}k)$ for lossy SPP mode [22]. In addition, as seen in Fig. 3, SPP mode is forbidden to propagate when the frequency is beyond the resonance frequency (ω_{sp}), so the integral upper limits of ∞ in Eqs. (10) and (11) could be replaced by ω_{sp} to conveniently calculate the PF in either form.

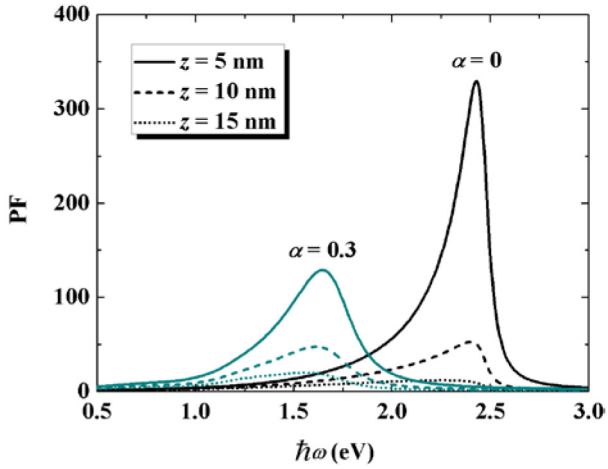

Fig. 5. Calculated PF spectra at the locations of z = 5 nm, 10 nm and 15 nm, for α = 0 and 0.3, respectively.

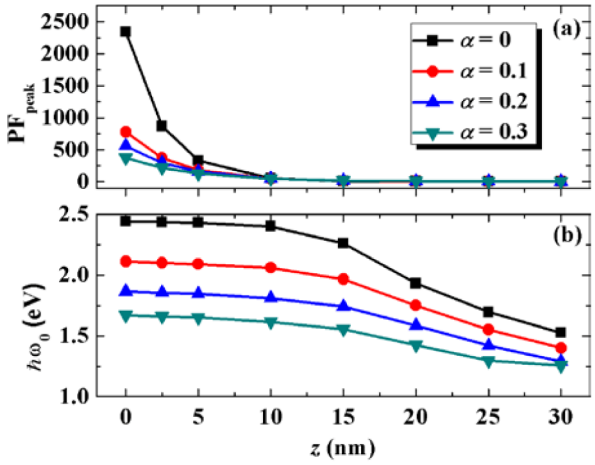

Fig. 6. Peak values PF_{peak} of PF spectra (a) and corresponding energies $\hbar\omega_0$ (b) at various locations of z = 0~30 nm for α = 0~0.3.

#176746 - $15.00 USD Received 24 Sep 2012; revised 14 Nov 2012; accepted 9 Dec 2012; published 4 Jan 2013

Figure 5 shows the PF spectra ($PF(\omega,z)$) at the locations of z = 5 nm, 10 nm and 15 nm beneath the Au(1-α)Si_3N_4(α) cermet waveguide with α = 0 and 0.3. As to the pure Au (α = 0), the PF spectrum at z = 15 nm is degraded dramatically compared with that at z = 5 nm, indicating that the plasmonic enhancement is limited in narrow space of only a few tens of nanometers. Meanwhile, the corresponding PF spectrum linewidth is significantly broadened. These phenomena, same as in Ref [22], can also be found in the other cermet waveguides (e.g., α = 0.3). But with increasing α, the PF spectrum peak is red-shifted at any location, and is notably reduced at z = 5nm due to the grain size effect that arouses stronger scattering loss with decreasing Au-NC size [13]. For more clarity, we plot the peak values (PF_{peak}) and the corresponding energies ($\hbar\omega_0$) at various locations of z = 0~30 nm in Fig. 6. It is seen that the plasmonic enhancement decays remarkably in the first ten nanometers and nearly to be 1 at z = 30 nm. Along with the PF decay, $\hbar\omega_0$ is firstly red-shifted a little but shows prominent changes after z>15 nm, as shown in Fig. 6(b), which may result from the evanescent property of electric field in the active layer.

Based on the above PF spectra, the PFs in the full integral form ($PF(z|\omega_0)$) can be numerically calculated. To maximize overall plasmonic enhancement under varied emission linewidths ($\Delta\omega$), the central frequency of the emitter (ω_0) should be matched with that of PF spectrum at the position where the strongest PF_{peak} is achieved. Clearly, this position should be at the cermet-emitter interface (z = 0 nm). But unfortunately, if the QDs approach very close to the waveguide (<5 nm), SE is almost completely coupled into lossy surface wave mode instead of SPP mode, leading to unfavorable luminescence quenching [32–34]. Therefore, a spacer is necessarily added between the cermet and the emitter [2,3]. Assuming that the spacer is 5 nm thick and its refractive index remains the same as that of the active layer, ω_0 should then be matched with the central frequency (ω_1) of PF spectrum at the spacer-emitter interface (z = 5nm), ceteris paribus. Then to evaluate overall plasmonic enhancement, $PF(z|\omega_0)$ is further averaged by the following equation:

$$PF_{ave} = 1 + \frac{1}{D_z}\int_s^{D_z} (PF(z \mid \omega_0) - 1)dz, \tag{17}$$

where s is the spacer thickness that is set 5 nm and thus $\omega_0 = \omega_1$, and D_z approximating 30 nm here is the decay length at which the peak value of PF spectrum decays to 1 within the active layer.

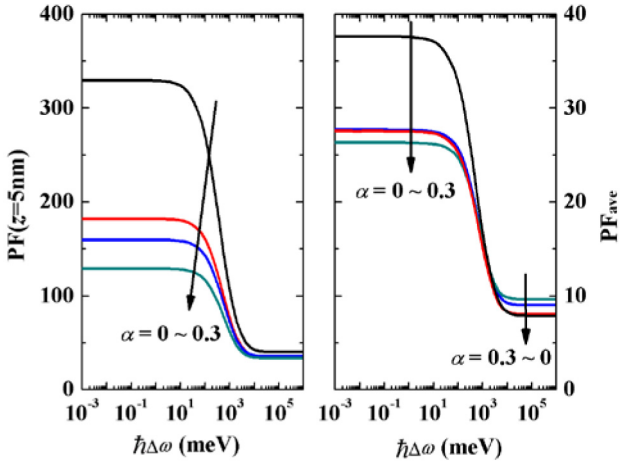

Fig. 7. Calculated PFs in the full integral form at z = 5 nm (a) and on average over the active layer (b) with varied emission linewidth ($\Delta\omega$) for α = 0~0.3; the central frequency of the emitter (ω_0) is matched with that of the PF spectrum (ω_1) at the spacer-emitter interface (z = 5 nm).

#176746 - $15.00 USD Received 24 Sep 2012; revised 14 Nov 2012; accepted 9 Dec 2012; published 4 Jan 2013

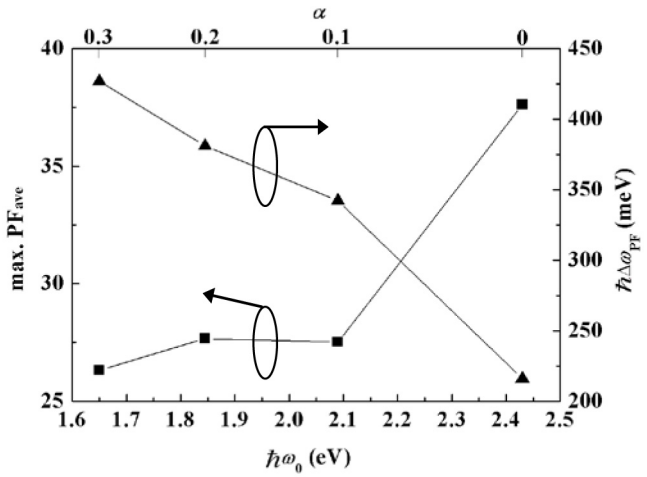

Fig. 8. Maximum PF_{ave} and PF spectrum linewidth at the spacer-emitter interface ($\Delta\omega_{PF}$) versus central emission frequency (ω_0) of the emitter for α = 0~0.3.

As shown in Fig. 7, due to the PF decay with distance, the calculated average PF (PF_{ave}) is much smaller than the PF at z = 5nm with $\hbar\Delta\omega = 10^{-3}$~$10^{6}$ meV. Specially, PF_{ave} drops to less than 10 when the emission linewidth exceeds ~0.1 eV. For narrow-linewidth emitters, increasing the doping fraction (α) would deteriorate both the PF at z = 5nm and PF_{ave} since additional loss is introduced due to the grain size effect of Au-NCs. It should be noted that the PF_{ave} curves for α = 0.1 and 0.2 overlap almost completely. This is because that besides introducing greater additional loss for decreased Au-NC size, increasing α would increase the real part of cermet permittivity ($\mathrm{Re}(\varepsilon_2)$) as shown in Fig. 2, which is yet helpful to improve PF. Since the grain size effect is dominant for the dielectric-doped cermet, tuning SPP resonance would be accompanied with PF degradation. However, for wide-linewidth emitters, such additional loss is helpful to obtain higher PF_{ave}. It could be understood that although such additional loss of cermet would lead to DOS spectral broadening and degrade the PF, the broadening of DOS spectrum would also enlarge the integration span and counterbalance the impact of reduced DOS value. In Fig. 8, with increasing α the maximum PF_{ave} decreases approximately linearly and the central emission frequency is lowered correspondingly in a wide range of $\hbar\omega_0$ = 2.43~1.65 eV. Meanwhile, the linewidth of PF spectrum at the spacer-emitter interface, denoted as $\Delta\omega_{PF}$, increases due to the grain size effect. However, in order to achieve the maximum PF_{ave}, the emission linewidth should be sufficiently narrow.

#176746 - $15.00 USD Received 24 Sep 2012; revised 14 Nov 2012; accepted 9 Dec 2012; published 4 Jan 2013

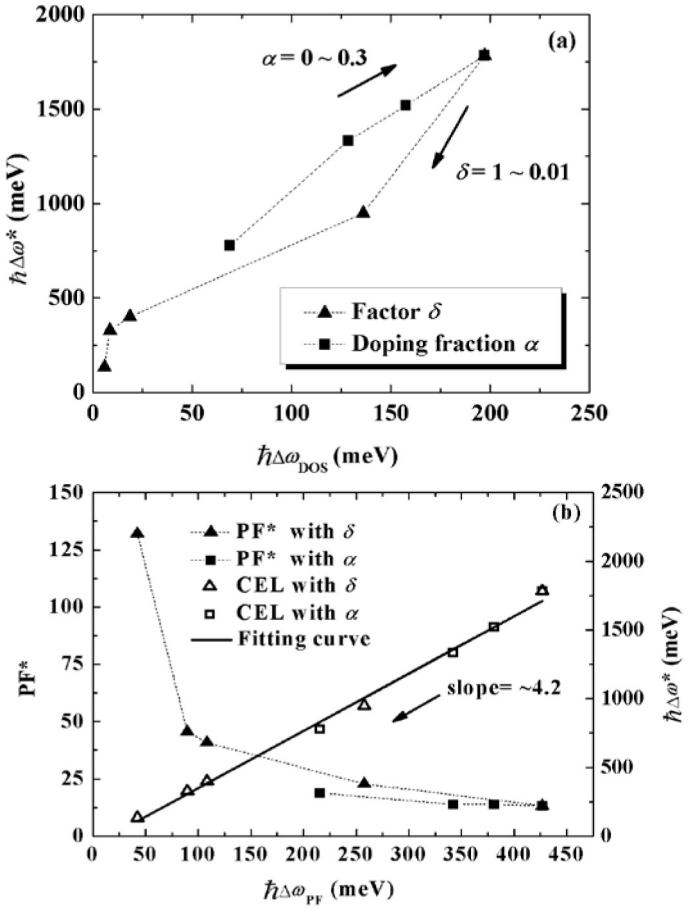

Fig. 9. Critical emission linewidth (CEL, $\Delta\omega^*$) versus DOS spectrum linewidth ($\Delta\omega_{DOS}$) under $\omega_k = \omega_1$ (a); critical emission linewidth (CEL, $\Delta\omega^*$) and corresponding PF_{ave} (PF*) versus PF spectrum linewidth ($\Delta\omega_{PF}$) at the spacer-emitter interface of z = 5nm (b), for α = 0~0.3 and for α = 0.3 with the imaginary part of its permittivity multiplied by a factor δ = 1~0.01, respectively.

Then, for finding out when it is "sufficiently narrow", we define the critical emission linewidth ($\Delta\omega^*$) as the one where the PF_{ave} drops to half of its maximum (PF*). If the emission linewidth is below $\Delta\omega^*$, it is considered to be sufficiently narrow for large plasmonic enhancement; otherwise the PF would be significantly degraded by wide emission linewidth. As shown in Fig. 9(a), with increasing α, $\Delta\omega^*$ and the DOS spectrum linewidth ($\Delta\omega_{DOS}$) under $\omega_k = \omega_1$ would also increase due to the grain size effect. And in Fig. 9(b), PF* decreases with broadening $\Delta\omega_{PF}$. The relation between $\Delta\omega^*$ and $\Delta\omega_{PF}$ looks positively linear. In order to achieve higher PF*, moreover, we take $Au(0.7)Si_3N_4(0.3)$ cermet for example, and multiply the imaginary part of its permittivity with a factor (δ = 1, 0.5, 0.1, 0.05 and 0.01) to reduce the waveguide loss on a larger scale. A similar positive relationship between $\Delta\omega^*$ and $\Delta\omega_{DOS}$ could also be seen in Fig. 9(a). And as shown in Fig. 9(b), ultrahigh PF could be obtained only when both the emission linewidth and the propagation loss of SPP mode could be dramatically reduced (e.g., $\hbar\Delta\omega_{PF}$<50 meV and $\hbar\Delta\omega^*$<140 meV). In addition, the relation between $\Delta\omega^*$ and $\Delta\omega_{PF}$ remains linear. By fitting all the values obtained so far, it could be expressed as $\hbar\Delta\omega^* \approx L(\hbar\Delta\omega_{PF}) = 4.2 \times \hbar\Delta\omega_{PF} - 69.2$ meV. This result is similar with that in our previous work based on metallic gratings, where a linear relation between the critical emission linewidth and the DOS spectrum linewidth was obtained [23]. But the slope was as small as

#176746 - $15.00 USD Received 24 Sep 2012; revised 14 Nov 2012; accepted 9 Dec 2012; published 4 Jan 2013

~0.55, which is mainly attributed to the definition of critical emission linewidth. For the study under metallic gratings, it was at a specific location near the waveguide that the critical emission linewidth was defined as the one corresponding to the crossing point of two *PF*-$\hbar\Delta\omega$ curves for lossy and lossless SPP modes. If the emission linewidth exceeded the critical linewidth, the PF of lossy SPP mode would be larger than that of lossless mode; namely, the broadening of PF or DOS spectrum due to the waveguide loss would be helpful for wide-linewidth QDs at the location. However, if the PFs are averaged over the active layer, the emission-linewidth requirement would be relaxed, because the PF spectrum within the active layer broadens away from the waveguide. It should be noted that the PF spectrum is the integral effect of all DOS spectra under different ω_k in Eq. (11), so $\Delta\omega_{PF}$ is wider than $\Delta\omega_{DOS}$.

According to the above results, some guidelines to achieve strong plasmonic enhancement could be summarized as follows:

(1) The central frequency of the emitter should be matched with that of PF spectrum at such a location where the highest PF is achieved.

(2) The emission linewidth of emitter should be matched to the PF spectrum linewidth, namely $\Delta\omega<\Delta\omega^*\sim L(\Delta\omega_{PF})$. Otherwise, broad emission linewidth will lead to significant PF degradation. It should be mentioned that if the active layer is thicker within the decay length (D_z) the emission linewidth of emitter could be broader.

(3) Both the emission linewidth and the SPP waveguide loss are the physical limitations to achieve ultrahigh PF_{ave}. As shown in Fig. 9(b), they need to be dramatically reduced. Such reduction could be achieved at low temperature as discussed in Ref [23]. Therefore, low-temperature emitters with strong plasmonic enhancement would be an interesting research subject. But this is beyond the scope of the paper. We are expecting some corresponding experimental investigations.

5. Conclusion

In summary, the plasmonic enhancement for different Au(1-α)Si_3N_4(α) cermet waveguides including pure Au is evaluated by utilizing the deduced PF in the full integral form ($PF(z|\omega_0)$), where both the DOS spectrum ($\rho(\omega_0-\omega_k)$) of SPP mode and the SE spectrum of emitter ($l(\omega-\omega_0)$) are involved. It is found that the cermet waveguides offer the advantages of tuning the SPP resonance whereas accompanied with the PF degradation due to the grain size effect, but in contrast, the emission linewidth and the broadening of PF spectrum ($PF(\omega,z)$) can markedly deteriorate the plasmonic enhancement. It is also found that the critical emission linewidth ($\Delta\omega^*$) is approximately linear to the linewidth of the highest PF spectrum ($\Delta\omega_{PF}$). These results suggest that both the emission linewidth and the PF spectrum linewidth should be dramatically reduced in order to achieve strong plasmonic enhancement.

Acknowledgments

This work was supported by the National Basic Research Program of China (No. 2011CBA00608, 2011CBA00303, 2011CB301803, and 2010CB327405) and the National Natural Science Foundation of China (Grant No. 61036010 and 61036011). The authors would like to thank Dr. Wei Zhang and Dr. Fang Liu for their valuable discussions and helpful comments.

#176746 - $15.00 USD Received 24 Sep 2012; revised 14 Nov 2012; accepted 9 Dec 2012; published 4 Jan 2013